Conjugation of Palmitic Acid Improves Potency and Longevity of siRNA Delivered via Endosomolytic Polymer Nanoparticles

By:

Samantha M. Sarett

Thesis

Submitted to the Faculty of the

Graduate School of Vanderbilt University

in partial fulfillment of the requirements

for the degree of

Master of Science

in Biomedical Engineering

December, 2014

Nashville, Tennessee

Approved:

Craig L. Duvall, Ph.D.

Hak-Joon Sung, Ph.D.

ACKNOWLEDGEMENTS

I would like to thank my advisor, Dr. Craig Duvall, whose ideas and expertise shaped this work and whose guidance was invaluable throughout its progress. From the beginning, his support motivated me to succeed and his advice and expertise guided my research. I would also like to thank all of the members of the Advanced Therapeutics Laboratory at Vanderbilt University for their constant help and encouragement. Particularly, I would like to thank Dr. Chris Nelson, whose prior successes motivated this work and who has assisted me in experiments, answered countless questions, and provided a wealth of relevant knowledge. I would also like to thank Martina Miteva and Kameron Kilchrist for their contributions to this work, as well as Kelsey Beavers, John Martin, Thomas Werfel, and Brian Evans for their support in experiments, scientific discussion, and life throughout my time at Vanderbilt.

In addition, I would like to thank Dr. Hak-Joon Sung and Dr. Scott Guelcher as well as the members of their groups for their expertise and assistance in my research. I would also like to thank Dr. Jeffrey Davidson and Dr. Fang Yu for their support in designing animal studies. I would additionally like to thank Dr. John McLean and his former student Dr. Jay Forsythe for help with matrix assisted laser desorption ionization mass spectrometry.

Dynamic light scattering was performed using a Zetasizer Nano-ZS Malvern Instruments Ltd in the Vanderbilt Institute of Nanoscale Sciences and Engineering (VINSE). Transmission electron microsopy was performed using a CM 20 TEM (supported by the NSF through grant NSF EPS 1004083) also through VINSE. This work was supported by the Vanderbilt School of Engineering, the NIH through the grant NIH R21EB012750 and the NSF through NSF CAREER BMAT 1349604 and a graduate research fellowship.

TABLE OF CONTENTS

Page

LIST OF FIGURES

Figure Page

Supplementary Figure

Chapter I

Introduction

Chronic Wounds

Impaired wound healing is a significant healthcare problem in the United States that affects more than 6.5 million people[1]. Patients with diabetes are ten times more likely to suffer amputation due to non-healing wounds, and the Center for Disease Control estimates that 1 in 3 of today's children will develop diabetes in their lifetime[2, 3]. It is anticipated that the prevalence of problematic skin wounds will parallel the expanding diabetes pandemic. Thus, there is an established, growing, and unmet clinical need for improved treatment of chronic wounds.

In normal wound healing, a coordinated combination of cellular infiltration, proliferation, and extracellular matrix deposition directs a transition from the initial inflammatory response at a site of injury to the process of tissue regeneration[4, 5]. Two cell types that are particularly relevant to this shift are fibroblasts and mesenchymal stem cells. Fibroblasts play a key role in wound remodeling via their proliferation, secretion of growth factors, extracellular matrix production, and promotion of angiogenesis[4]. However, fibroblasts isolated from chronic wounds show a decrease in proliferation rate and a diminished response to various cytokines[4, 6]. While the mechanism for this alteration in fibroblast behavior has not been identified, this indicates that mere delivery of growth factors will be insufficient to fully restore normal fibroblast behavior at the site of chronic wounds.

MSCs are central regulators of wound healing; they modulate the inflammatory response and release bioactive factors that influence the migration, proliferation, and phenotype of nearby cells. Additionally, the capacity of MSCs to differentiate into various tissue-forming cell types

endows them with particular value in functional tissue regeneration[5]. Modulating the characteristics and activities of cells essential to the wound healing process, such as fibroblasts and MSCs, is a potentially high-impact strategy for chronic wound treatment.

Due to the complex nature of wound healing, a variety of physiological abnormalities can contribute to impaired healing. However, inadequate angiogenesis and the resulting deficiencies in oxygen and nutrient delivery to developing tissue have been identified as key problems in chronic wounds[4]. The inhibition of prolyl hydroxylase 2 (PHD2) in cells recruited to the site of wound healing has emerged as a powerful strategy to promote angiogenesis. PHD2 is an endogenous negative regulator of the transcription factor hypoxia-inducible factor-1α (HIF-1α)[7]. Potent inhibition of PHD2 results in a large up-regulation of HIF-1α and its downstream genes VEGF, fibroblast growth factor 2 (FGF-2), endothelial nitric oxide synthase (eNOS), angiopoietin (ANGPT), and stromal cell-derived factor 1 (SDF-1)[8, 9]. These factors orchestrate both formation and maturation of vessels and, in the case of SDF-1, recruit endothelial progenitors that further promote local vasculogenesis[10]. This work aims to optimize a therapeutic strategy for PHD2 inhibition that will prompt angiogenesis in non-healing wounds and therefore promote wound resolution.

siRNA Therapeutics

Physiological gene inhibition presents a powerful alternative to typical small molecule drugs, as the suppression of a strategically selected gene allows for simultaneous modulation of a myriad of downstream targets and facilitates a broad and coordinated therapeutic effect. Small interfering RNA (siRNA) therapeutics are capable of potently and specifically silencing a gene of interest and therefore show great promise for treatment of a broad range of disease states,

including that of impaired wound healing. However, clinical application of siRNA remains limited by barriers to delivery to its site of action in the cellular cytoplasm. siRNA has a short half-life *in vivo*, is incapable of effectively translocating the cellular membrane, and faces lysosomal degradation upon endocytosis. Strategies to address these issues are diverse, encompassing a wide range of carriers and conjugates[11]. Most relevant to this work are methods that hydrophobize the siRNA delivery system, particularly via direct conjugation of a hydrophobic moiety.

The conventional and most utilized approach for delivery of siRNA is via electrostatic condensation into nanocarriers using polycationic polymers or lipids. Optimized polymeric and lipid carriers can protect the siRNA against degradation and transport it into the cell[12]. The incorporation of endosomolytic moieties like propyl(acrylic acid) can also facilitate endosomal escape[13]. However, these carrier systems can elicit an immune response and cytotoxicity at high concentrations[14]. Increasing gene silencing potency and enabling the use of lower doses of the delivery system thus enhances the likelihood of siRNA's therapeutic application. A promising strategy to accomplish this aim is via hydrophobization of the carrier or of the siRNA itself.

Increased hydrophobicity of cationic polymer siRNA delivery systems has been shown to correspond to improvements in gene silencing. Hydrophobization of the cationic carrier poly(ethylene imine) via conjugation of lipids to the polymer maintains silencing efficacy while reducing cytotoxicity, although the lipid chains begin to negatively impact gene silencing at a threshold chain length[15]. Additionally, more hydrophobic poly(β-amino ester)-based delivery vehicles were shown to achieve greater transfection than comparable counterparts[16]. Developing a balance between hydrophobic content and cationic content of an siRNA carrier could allow for enhanced uptake and silencing efficiency at a lower polymer dose[17].

Hydrophobization of the siRNA itself is another approach to facilitate increased interaction with the cellular membrane and thus improve uptake. Lipid-conjugated siRNA has been explored as a means of gene silencing both with and without an additional carrier[18, 19]. It was found that palmitic acid conferred increased stability to siRNA while also enhancing cellular penetration and gene silencing[20, 21]. Palmitic acid-conjugated siRNA (siRNA-PA) was additionally found to be superior to various aromatic groups and additional lipidic moieties in gene silencing efficacy and cellular internalization [22, 23]. While siRNA-PA exhibited some silencing activity without a carrier system, it was most efficacious in combination with the commercial lipidic vector Lipofectamine2000.

Approach

Our lab has previously reported on biomaterial scaffold-based delivery of siRNA-loaded endosomolytic polymer nanoparticles to promote angiogenesis at wound sites. The siRNA delivered was designed against PHD2 and promoted therapeutic neovascularization of ischemic tissues, enhanced tissue repair, and facilitated tissue scaffold vascularization and integration[24, 25]. This work aims to optimize the design of the siRNA nanoparticle system and reduce the polymer dose required to elicit potent and sustained gene silencing. Our approach is to conjugate PA directly to siRNA, thereby improving its stability as well as increasing the hydrophobicity of the siRNA-loaded nanoparticles. It is anticipated that the conjugation of PA will broaden the therapeutic index of this carrier system and increase the likelihood of successful translation of this system in wound healing applications.

Chapter II

Conjugation of Palmitic Acid Improves Potency and Longevity of siRNA Delivered via Endosomolytic Polymer Nanoparticles

Abstract

Clinical translation of siRNA therapeutics has been limited by the inability to effectively overcome the rigorous delivery barriers associated with intracellular-acting biologics. Here, in order to address both potency and longevity of siRNA gene silencing, siRNA conjugated to palmitic acid (siRNA-PA) was paired with pH-responsive micellar nanoparticle (NP) carriers in order to improve siRNA stability and endosomal escape, respectively. Conjugation to hydrophobic PA improved NP loading efficiency relative to unmodified siRNA, enabling complete packaging of siRNA-PA at a lower polymer:siRNA ratio. PA conjugation also increased intracellular uptake of the nucleic acid cargo by 35-fold and produced a 3.1-fold increase in intracellular half-life. The higher uptake and improved retention of siRNA-PA NPs correlated to a 2- to 3-fold decrease in gene silencing IC_{50} in comparison to siRNA NPs in both mouse fibroblasts and mesenchymal stem cells for both the model gene luciferase and the therapeutically relevant gene PHD2. PA conjugation also increased longevity of silencing activity, as indicated by an increase in silencing half-life from 24 hours to 186 hours. Thus, conjugation of PA to siRNA paired with endosomolytic NPs is a promising approach to enhance the functional efficacy of siRNA in tissue regenerative and other applications.

Keywords

Gene knockdown, endosomolytic nanoparticle, siRNA conjugation

Introduction

Therapeutic application of RNA interference provides the potential to potently and specifically suppress transcription factors, subsets of kinases, and other signaling molecules that are traditionally considered "undruggable". Unfortunately, achieving successful *in vivo* delivery of siRNA has proven a complex and difficult challenge, impeding medicinal translation of siRNA therapeutics. siRNA has a short half-life due to nuclease susceptibility, rapid renal clearance if injected intravenously, and an inability to translocate the membranes that make up the outer cell surface and the vesicles of the endolysosomal recycling/degradation pathways[11, 26, 27]. Numerous and varied strategies have been developed in attempts to address these delivery obstacles, including modifications to the siRNA backbone, the use of lipids and polymers as carrier systems, and the conjugation of siRNA to cell-penetrating/cell-binding peptides, antibodies, dendrimers, and lipid-like molecules[11, 15, 28-31]. Tremendous progress has been made, especially in the application of lipid nanoparticles for delivery of siRNA against hepatic targets, but widespread medicinal application of siRNA remains a distant goal[32, 33]. Thus, there is a continued need to better elucidate the ideal siRNA chemistry and its potential synergism with polymeric- and lipid-based carriers, with the goal of discovering combinations that will expand the therapeutic use of siRNA for a broader set of clinical indications.

Work from our lab and others has focused on diblock copolymers that can package and deliver siRNA to the cytoplasm, facilitated by pH-dependent membrane disruptive activity that promotes endosomal escape[17, 24, 29, 34]. In the current work, we sought to improve the performance of siRNA formulations with these promising polymers, with the goal of improving efficacy and longevity of action such that functional effects can be achieved at a reduced polymer/siRNA dose. Lessening the dose of the carrier is anticipated to be advantageous in

reducing nonspecific side effects, as high doses of both cationic lipids and polymers can induce production of inflammatory cytokines and interferons, global changes in gene expression, and toxicity[11, 14, 30, 35].

Hydrophobization of nucleic acid delivery systems has been demonstrated to enhance carrier stability and transfection efficiency in a broadly applicable manner[15-17, 36]. The conjugation of hydrophobic moieties to siRNA can increase siRNA nuclease resistance and enhance cellular internalization without detrimentally impacting gene silencing activity[20, 23]. Direct conjugation of siRNA to cholesterol and α-tocopherol improves gene silencing efficacy *in vivo*, especially when the target site is the liver and after incubation of the conjugated siRNA with lipoproteins[19, 37, 38]. Conjugation of palmitic acid (PA) to siRNA has shown particular promise as a modification strategy to improve siRNA stability, cellular penetration, and gene silencing[23]. PA is an endogenous post-transcriptional modification commonly found on membrane-associated signaling proteins. While PA is involved in a wide variety of cellular functions, it is especially believed to influence protein-membrane interactions as well as protein uptake and intracellular trafficking[39-41]. Motivated by the inherent effects of PA on membrane binding and translocation, PA-modified siRNA has been recently tested as an approach to enhance gene silencing in comparison to unmodified siRNA or siRNA conjugated to cholesterol in cancer cell lines *in vitro*[20, 23]. In these studies, PA conjugation was demonstrated to enhance knockdown of siRNA delivered via Lipofectamine 2000 (a commercial transfection reagent with established cytotoxicity) and also to enable some gene silencing in the absence of a transfection reagent at high (micromolar) doses[14, 20].

These promising siRNA conjugate results motivated the current study, which was aimed at testing siRNA-PA conjugates for delivery via endosomolytic polymer-based nanoparticles and

at assessing PA conjugates in different cell lines relevant to regenerative medicine applications. The ultimate goal of these studies is to enhance the therapeutic potency in order to minimize the quantity of polymeric carrier and siRNA required, thus reducing the potential for nonspecific effects. We have previously delivered polymeric siRNA nanoparticles from porous, biodegradable polyester urethane (PEUR) scaffolds to achieve tunable and potent gene silencing[24, 25]. This approach for local siRNA delivery has shown tremendous potential in applications for tissue regeneration, especially through local silencing of prolyl hydroxylase domain protein 2 (PHD2) to promote wound healing. PHD2 negatively regulates hypoxia inducible factor 1α, a pro-angiogenic transcription factor, and scaffold-based delivery of PHD2 siRNA activates a pro-angiogenic, pro-proliferation program[25, 42, 43]. The current studies were designed to assess the potential of PA conjugation for enhancing the potency and longevity of gene silencing of siRNA for ultimate application in wound healing.

Experimental Methods

Materials: Amine-modified single-stranded DNA (modification at 5' end) or Dicer substrate siRNA (modification at 3' end) and complementary single-stranded Cy5-modified DNA or unmodified Dicer substrate siRNA were obtained from Integrated DNA Technologies (Coralville, Iowa). The pGreenFire1-CMV plasmid was obtained from System Biosciences (Mountain View, CA), and packaging plasmids pMDLg/pRRE, pRSV-Rev, and pMD2.G were purchased from Addgene (Cambridge, MA). Lipofectamine 2000 and NucBlue Fixed Cell ReadyProbes were purchased from Life Technologies (Grand Island, NY). RNEasy spin columns were obtained from Qiagen (Venlo, Netherlands), and the iScript cDNA Synthesis Kit from Bio-Rad (Hercules, CA). NIH-3T3s and HEK-293Ts were obtained from ATCC (Manassas, VA), and mouse marrow stromal cells (C57Bl/6-TgNs) were purchased from Jackson Laboratory (Bar

Harbor, ME). Propylacrylic acid was synthesized as previously reported[1,2]. All other reagents were purchased from Sigma-Aldrich (St. Louis, MO).

Oligonucleotide-PA Synthesis and Characterization: Single-stranded amine-modified oligo was reacted with 100-fold molar excess of PA *N*-hydroxysuccinimide ester pre-dissolved at 40 mM in *N*,*N*-dimethylformamide (DMF). The reaction was carried out for 18 hours at room temperature in 45% water, 45% isopropyl alcohol, and 10% DMF. The oligo-PA was purified by reversed-phase HPLC using a Clarity Oligo-RP column (Phenomenex, Torrence, CA) under a linear gradient from 95% water (50 mM triethylammonium acetate), 5% methanol to 100% methanol. The conjugate molecular weight was confirmed using MALDI-TOF mass spectrometry (Voyager-DE STR Workstation, Grand Island, NY) using 50 mg/mL 3-hydroxypicolinic acid in 50% water, 50% acetonitrile with 5 mg/mL ammonium citrate as a matrix. The yield of the oligo-PA was quantified based on absorbance at 260 nm. The purified oligo-PA was annealed to its complementary strand to generate Cy5-modified DNA-PA or siRNA-PA. Conjugation and annealing was also confirmed via agarose gel electrophoresis.

Oligonucleotide-loaded Nanoparticle (NP) Synthesis and Characterization: A diblock copolymer composed of a homopolymer of 2-(dimethylamino) ethyl methacrylate (DMAEMA) blocked with a random copolymer of DMAEMA, 2-propylacrylic acid (PAA), and butyl methacrylate (BMA) was synthesized using reversible addition-fragmentation chain transfer (RAFT) polymerization as described previously[24, 29]. Assembly of NPs was triggered by dissolving polymer in 100% ethanol, followed by slow addition of PBS or water via syringe pump. siRNA or DNA (with or without PA) was mixed with NPs and allowed to electrostatically condense for 30 minutes. Dynamic light scattering (DLS; Zetasizer Nano-ZS Malvern Instruments Ltd., Worcestershire, U.K.) and transmission electron microscopy (TEM; FEI

Tecnai Osiris, Hillsboro, OR) were used to analyze size and zeta potential of oligo-loaded NPs. Gel electrophoresis was used to test loading efficiency at varied amine:phosphate (N:P) ratios. A red blood cell hemolysis assay[44] was used to determine pH-dependent membrane disruptive activity of oligo NPs as a marker for endosomal escape functionality.

Production of Stable Luciferase-Expressing Cell Lines: To produce lentivirus, the pGreenFire1-CMV plasmid and packaging plasmids pMDLg/pRRE, pRSV-Rev, and pMD2.G were transfected into HEK-293Ts using Lipofectamine 2000. Media was changed after 24 hours and supernatant containing lentivirus was collected at 48 and 72 hours. Viral supernatant was added directly to NIH-3T3s with 6 μg/mL polybrene or mMSCs with 60 μg/mL protamine sulfate. Media was changed after 24 hours. Lentiviral transduction efficiency was evaluated by GFP expression as analyzed by flow cytometry (BD LSR II Flow Cytometer, San Jose, CA).

Luciferase Silencing: NIH-3T3s or mMSCs were treated with siRNA NPs or siRNA-PA NPs; the siRNA was either designed against the luciferase gene (luc siRNA) or was a scrambled sequence (scr siRNA). Cells were treated in 10% serum for 24 hours before imaging with an IVIS 200 imaging system (Caliper Life Sciences, Hopkinton, Massachusetts). Unless otherwise noted, an N:P ratio of 4:1 was used. In the investigation on longevity of luciferase silencing, the media was changed after 12 hours of treatment to 2% serum to prevent cellular overgrowth.

PHD2 Gene Silencing: NIH-3T3s were treated with siRNA NPs or siRNA-PA NPs at an N:P ratio of 4:1 as described above except for using prolyl-hydroxylase 2 (PHD2) siRNA. Cells were treated in 10% serum for 24 hours and then incubated for 24 hours, and the degree of PHD2 knockdown was quantified by real time polymerase chain reaction (RT-PCR) using the ΔΔCt method and normalizing to glyceraldehyde 3-phosphate dehydrogenase (GAPDH).

Cellular Uptake and Retention: NIH-3T3s were treated with Cy5-labeled DNA NPs or DNA-PA NPs in 10% serum for 12 hours at 12.5 nM. To measure retention with minimal dilution effects due to cell proliferation, media was then changed to 2% serum, and cells were cultured for up to an additional 72 hours. Intracellular fluorescence was quantified using flow cytometry at 12, 36, 60, and 84 hours. Extracellular membrane-bound fluorescence was quenched with Trypan Blue. For confocal microscopy imaging studies, NIH-3T3s were treated with 25 nM Cy5-labeled DNA NPs or DNA-PA NPs in 10% serum for 12 hours before media was changed to 2% serum. Cell nuclei were stained with DAPI (using NucBlue Fixed Cell ReadyProbes), and cellular fluorescence was imaged using confocal microscopy at 12, 36, and 60 hours.

To assess the mechanism of uptake of PA-conjugated oligo NPs, NIH-3T3s were pre-treated for 30 minutes with either Dynasore (5 μM), 5-(N-ethyl-N-isopropyl)amiloride (EIPA) (5 μM), or cytochalasin D (50 μM), which are inhibitors of clathrin/caveolin-mediated endocytosis, macropinocytosis, and caveolin-mediated endocytosis/macropinocytosis, respectively. Cy5-labeled DNA-PA NPs were then added at 50 nM, and the cells were incubated with both the inhibitors and NPs for 4 hours in 10% serum. Intracellular fluorescence was then quantified using flow cytometry with extracellular fluorescence quenched with Trypan Blue.

Results

Synthesis and Characterization of Oligo-PA NPs: PA-conjugated single-stranded oligos were successfully purified from the reactants via HPLC, and the desired products were confirmed by MALDI-TOF analysis (Figure 1) and also by an upward shift of the PA-siRNA band in comparison to the unmodified siRNA band on an agarose gel (Figure 3). Unmodified siRNA showed full loading into the diblock polymer NPs at an N:P ratio of 6:1, while PA-modified

siRNA was fully loaded at a ratio of 4:1 (Figure 2). Oligo-PA NPs were ~10 nm larger than unmodified oligo NPs (48 nm vs. 38 nm), as demonstrated by DLS and TEM (Figure 3). Zeta potential was equivalent between oligo-PA NPs and unmodified oligo NPs. No difference in pH-dependent membrane disruptive activity (i.e., as a measure of endosomolytic behavior) was detected between unmodified oligo NPs and oligo-PA NPs (Figure S1).

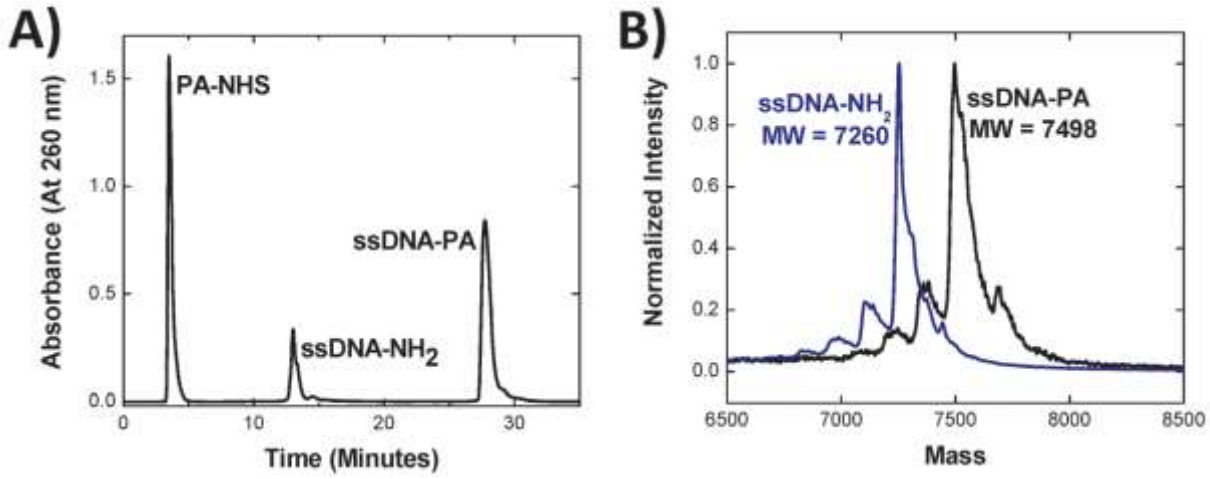

Figure 1. *Purification of PA-conjugated oligo. A) HPLC separation of PA-conjugated oligo from unreacted oligo, PA-NHS. B) Molecular-weight confirmation by MALDI-TOF mass spectrometry, normalized to maximum intensity for each measurement.*

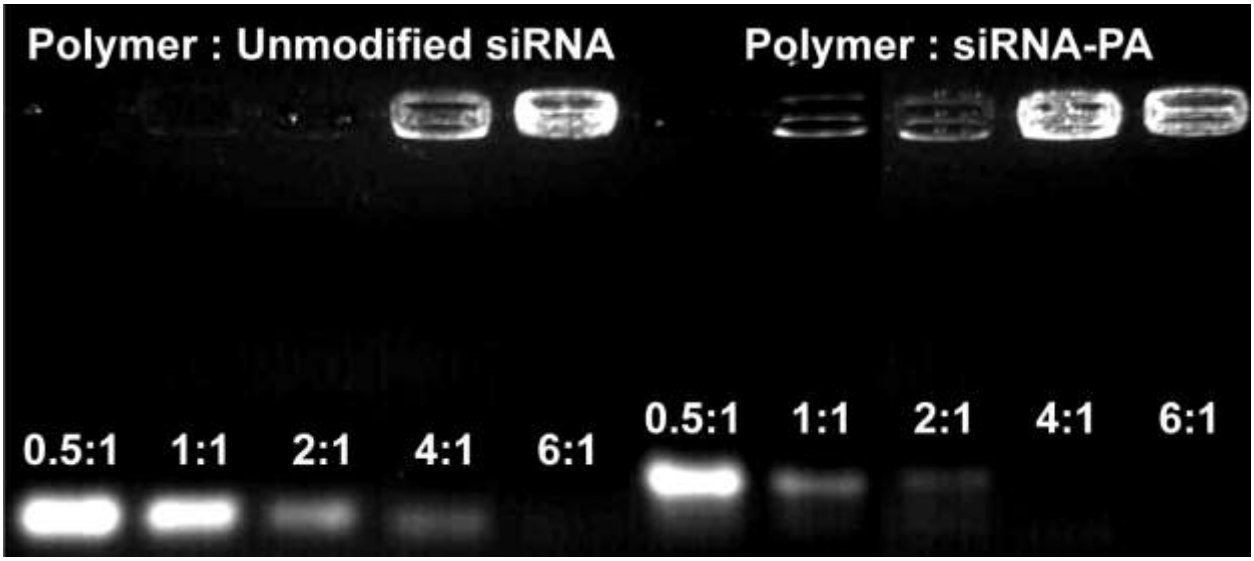

Figure 2. *The siRNA-PA conjugate efficiently loads into NPs at a lower N:P ratio than unmodified siRNA. siRNA-PA complexed completely at an N:P ratio of 4:1, unmodified siRNA at 6:1. An upward shift in migration time is seen for the PA-modified siRNA, further confirming successful conjugation.*

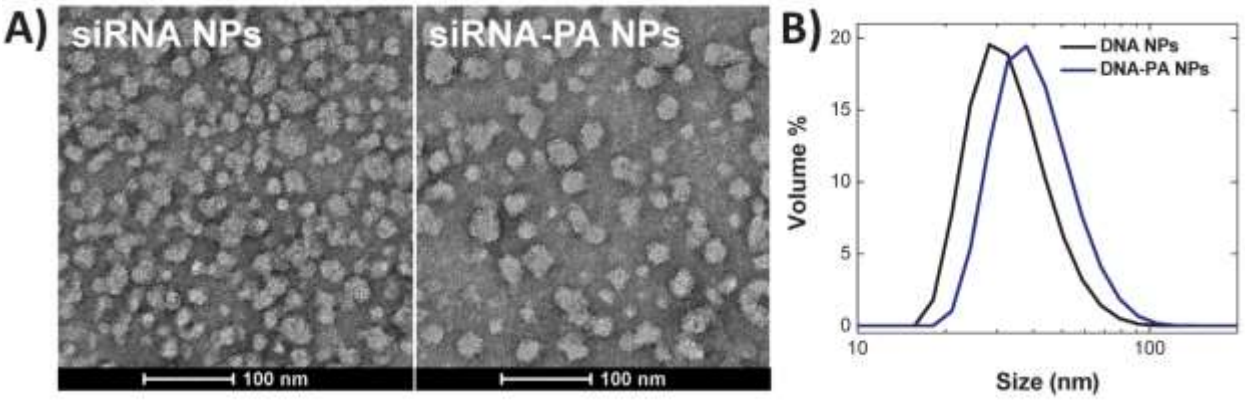

Figure 3. *Oligo-PA NPs have an approximately 20% larger hydrodynamic diameter than oligo NPs. A) TEM images of siRNA NPs and siRNA-PA NPs. B) DLS measurement of DNA NPs ($z_{average}$ diameter = 40 nm, PDI = 0.10) and DNA-PA NPs ($z_{average}$ diameter = 48 nm, PDI = 0.07).*

Gene Silencing Efficacy of siRNA-PA NPs: The influence of the difference in loading efficiency (i.e., N:P ratio required for full packaging) between unmodified and PA-modified siRNA was also investigated for gene silencing. While luc NPs showed a significant increase in luciferase silencing between a ratio of 4:1 and 6:1, no difference was seen in luc-PA NPs between these two different N:P ratios (Figure 4). Greater cytotoxicity, as evaluated by the scrambled controls, was seen at 6:1 in comparison to 4:1 demonstrating the impact of achieving more efficient loading and activity with a smaller quantity of polymeric carrier (Figure S2). Superior silencing was detected for luc-PA NPs in comparison to luc NPs at all N:P ratios.

At a fixed N:P ratio of 4:1, increased gene silencing bioactivity of luc-PA NPs over luc NPs was apparent in both mouse fibroblasts (NIH-3T3s) and mMSCs (Figure 5). The IC_{50} was

calculated based on equation 1 where y is the fraction luciferase activity, x is the concentration in nM, and b is a fit parameter.

Equation 1: $$y = \frac{-1}{(1+(\frac{x}{IC_{50}})^{b})} + 1$$

The IC_{50} of luc-PA NPs was 2.2-fold and 3.1-fold lower than that of luc NPs in the fibroblasts and the mMSCs, respectively, indicating that siRNA conjugation to PA significantly improves the gene silencing potency for a given N:P ratio. No significant difference in cytotoxicity was seen in the scr NPs compared to the scr-PA NPs. No significant cytotoxicity was seen below a 40 nM dose of siRNA NPs in the fibroblasts, and no significant cytotoxicity was seen at any of the siRNA NP doses tested in the mMSCs. No cytotoxicity was detected for any siRNA-PA NP doses tested in the fibroblasts or mMSCs.

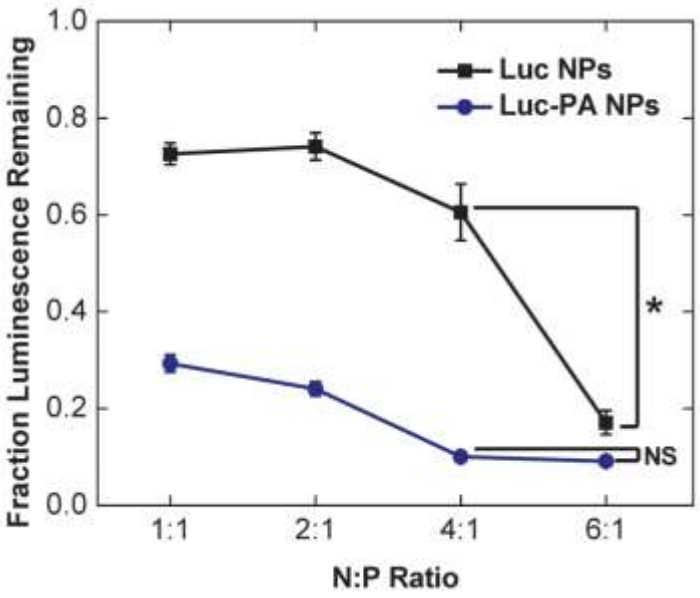

Figure 4. *Superior luciferase silencing at a lower N:P ratio using luc-PA siRNA vs. luc siRNA NPs. Increasing the N:P ratio above 4:1 did not improve luc-PA NP silencing. These studies were done at 40 nM siRNA treatment for 24 hours in NIH-3T3 fibroblasts. Data are normalized to scrambled controls.*

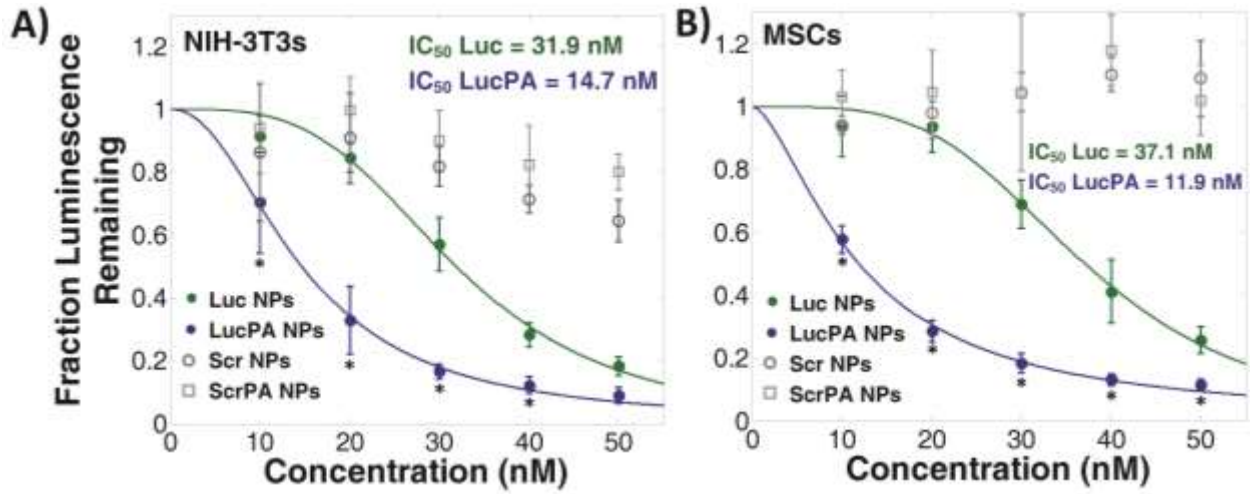

Figure 5. *Luc-PA NPs exhibited superior luciferase silencing vs. luc NPs at a range of doses. A) In NIH-3T3 fibroblasts, the IC_{50} of luc NPs was 31.9 nM and of luc-PA NPs was 14.7 nM. B) In mouse MSCs, the IC_{50} of luc NPs was 37.1 nM and of luc-PA NPs was 11.9 nM. *$p<0.05$ for luc-PA NP silencing in comparison to luc NP silencing. Data are normalized to untreated cells. Small relative decreases in signal in NIH-3T3s at higher doses of the scr NPs are indicative of mild cytotoxicity.*

The impact of PA modification on efficiency of silencing of the therapeutically-relevant gene PHD2 was also investigated. PHD2-PA NPs significantly enhanced gene silencing in comparison to PHD2 NPs when evaluated by RT-PCR (Figure 6). In fibroblasts, the IC_{50} of PHD2-PA NPs was 2.3-fold lower than that of PHD2 NPs. These data agree well with the data acquired using luc siRNA, confirming that the bioactivity gained through PA conjugation is consistent across different siRNAs.

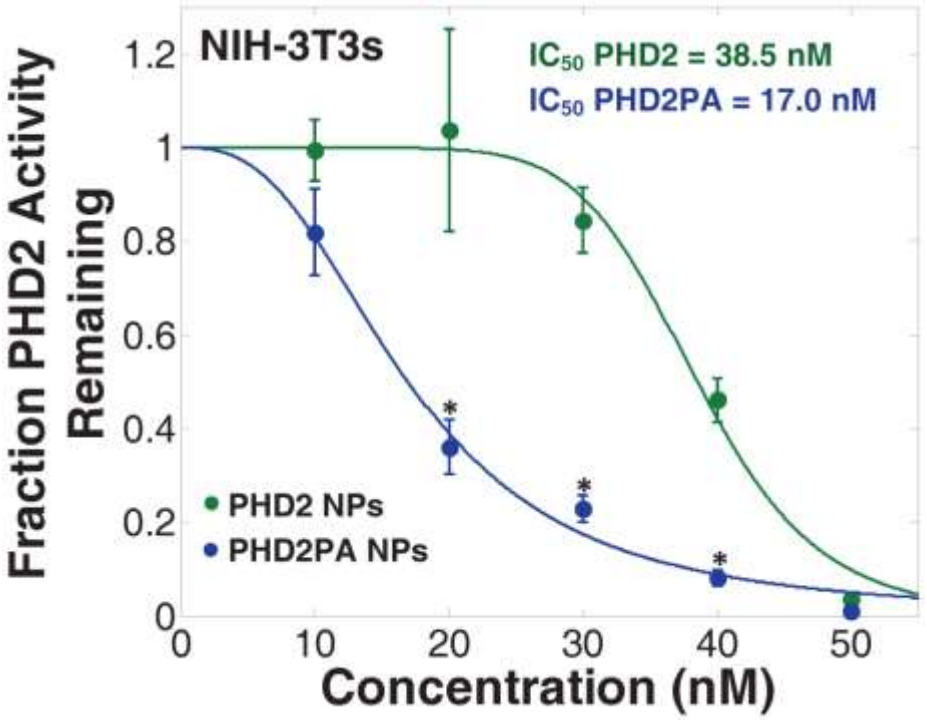

Figure 6. *PHD2-PA NPs exhibited superior silencing vs. PHD2 siRNA NPs at a range of doses. In NIH-3T3 fibroblasts, the IC_{50} of PHD2 NPs was 38.5 nM and of PHD2-PA NPs was 17.0 nM. *p<0.05 for PHD2-PA NP silencing in comparison to PHD2 NP silencing. Data are normalized to scrambled controls.*

Cellular Uptake and Retention of Oligo-PA NPs: To mechanistically explore the improved bioactivity achieved through PA conjugation, the cellular uptake and retention of fluorescently modified DNA NPs or DNA-PA NPs were evaluated by flow cytometry at an N:P of 4:1. The intracellular fluorescent intensity of fibroblasts treated with DNA-PA NPs was 35-fold higher than those treated with the same dose of DNA NPs (Figure 7A). The intracellular half-life of the DNA vs. the DNA-PA was also investigated by monitoring the intracellular fluorescence over time after treatment removal and fitting the data to equation 2 where y is the fluorescence, y_0 the initial fluorescence measured at the time of treatment removal, x is the time in hours, and λ is related to the half-life $t_{1/2}$ by equation 3. The intracellular half-life of DNA-PA was found to be 3.1-fold higher than that of unmodified DNA.

Equation 2: $y = y_0(e^{(-\lambda x)})$ **Equation 3**: $t_{1/2} = \frac{\ln(2)}{\lambda}$

In support of the flow cytometry data, confocal microscopy revealed visibly increased fluorescence of fibroblasts treated with DNA-PA NPs in comparison to DNA NPs (Figure 7B). The overexposure of the images depicting DNA-PA NP uptake was necessary to demonstrate the uptake of DNA NPs under the same imaging settings and results from the large difference in uptake of the fluorescently labeled siRNA between the two treatments. Additionally, microscopy images at 0, 24, and 48 hours post-removal of treatment supported the flow cytometry results, demonstrating better retention of PA conjugates over time. Importantly, untreated cells showed no fluorescence when imaged using the same microscope settings (Figure S3).

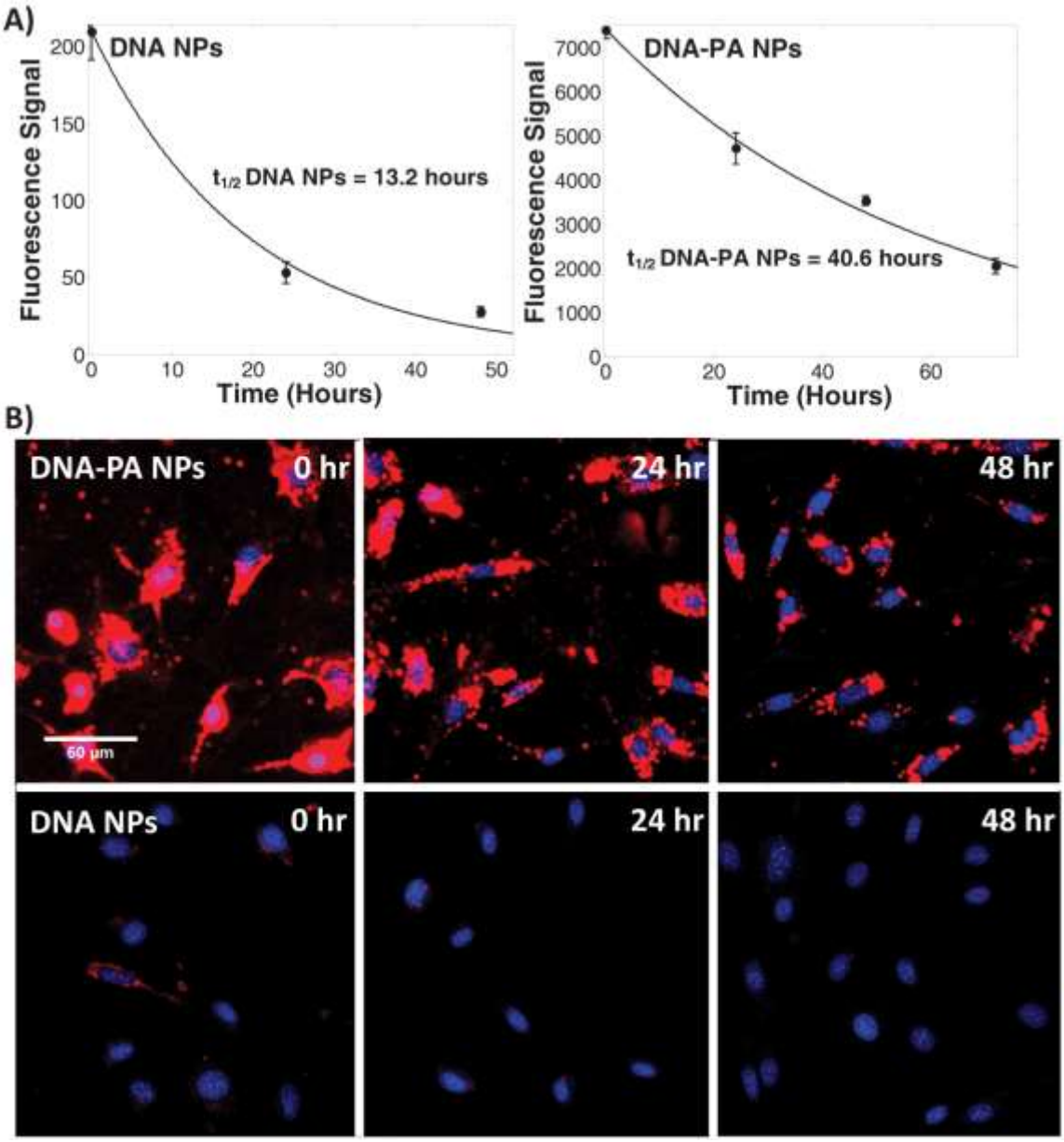

Figure 7. *A) Intracellular fluorescence was higher and more sustained after treatment with DNA-PA NPs vs. DNA NPs. Quantified by flow cytometry in NIH-3T3s, intracellular half-life of Cy5-labeled DNA NPs is 13.2 hours and of Cy5-labeled DNA-PA NPs is 40.6 hours. Initial fluorescent intensity of DNA-PA NPs is ~35 times that of DNA NPs. Data are normalized to no treatment. B) Confocal microscopy images show increased uptake of DNA-PA NPs vs. DNA NPs. Images are at 0, 24, and 48 hours of incubation post-removal of a 12 hour treatment.*

Next uptake pathway inhibitors were used to investigate the uptake mechanism of DNA-PA NPs in fibroblasts. EIPA, an amiloride analog and inhibitor of macropinocytosis, and cytochalasin D, which disrupts actin filament formation and thus impedes both caveolae-mediated uptake and macropinocytosis, significantly inhibited uptake of the DNA-PA NPs (Figure 8). Dynasore, which blocks a dynamin GTPase necessary for formation of all clathrin-coated vesicles and for uptake through caveolae, had no effect on uptake of DNA-PA NPs.

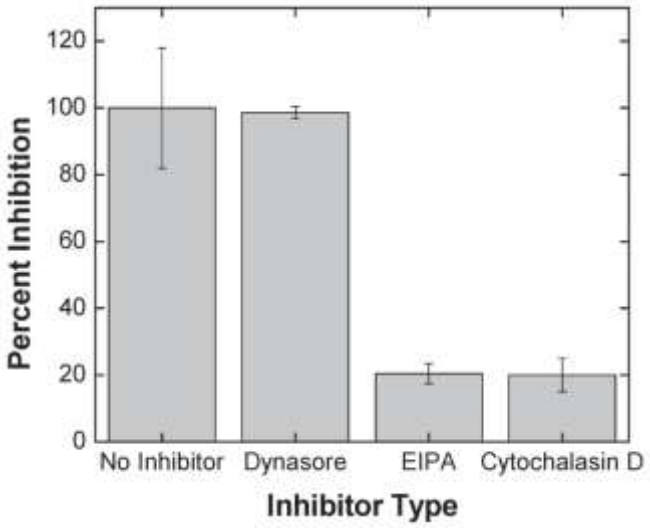

Figure 8. *Cellular uptake, as measured by intracellular fluorescence, of DNA-PA NPs was inhibited by EIPA and cytochalasin D but not Dynasore. Quantified by flow cytometry in NIH-3T3s and normalized to a no inhibitor control (set to 100%).*

Longevity of Gene Silencing of siRNA-PA NPs: The longevity of gene silencing of luc-PA NPs in comparison to unmodified luc NPs was investigated in NIH-3T3 fibroblasts. The duration of luciferase silencing with luc-PA NPs was increased in comparison to luc NPs. In cells treated by luc NPs, luciferase activity returned to equivalent to that of untreated cells by 72 hours, while cells treated with luc-PA NPs exhibited no decrease in silencing between 48 and 72 hours

(Figure 9). After 7 days, cells treated with luc-PA NPs still showed 40% of the silencing effect detected at 24 hours (28% overall luciferase silencing in comparison to cells treated with scr-PA NPs). Quantification of silencing half-life (based on percentage of silencing measured upon treatment removal at 24 hours) using Equations 2 and 3 revealed a half-life of 24 hours post-treatment removal for unmodified luc NPs in comparison to 186 hours for luc-PA NPs. This functional longevity of action corresponds to the increased intracellular half-life of DNA-PA compared to unmodified DNA.

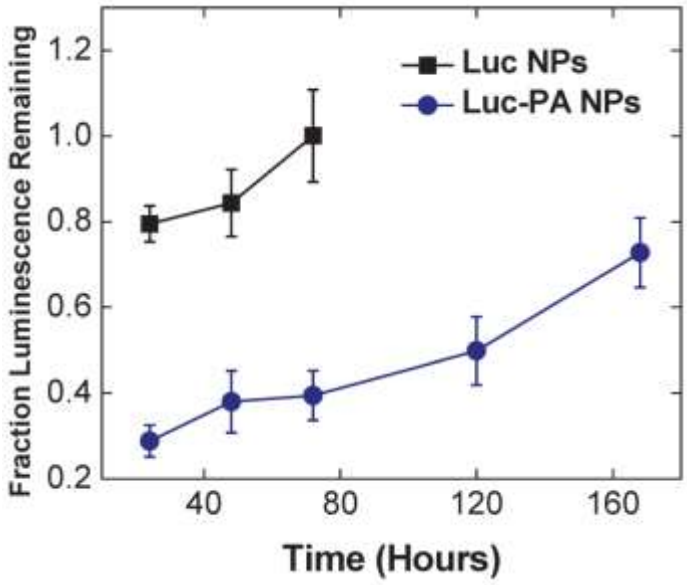

Figure 9. *Luc-PA NPs silenced more effectively and over an increased duration relative to luc NPs. In NIH-3T3s treated at 30 nM, luc NP-treated cells recovered from luciferase knockdown by 72 hours while at 168 hours, luc-PA NP-treated cells still showed partial silencing. Normalized to scrambled controls.*

Discussion

Direct conjugation of siRNA to targeting ligands, lipophilic moieties, or carrier molecules is a promising approach to enhancing knockdown efficacy and/or reducing the need for additional

transfection reagents[38, 45, 46]. Palmitic acid has shown particular promise for increasing resistance to nuclease degradation, cellular uptake, and gene silencing in initial *in vitro* tests using commercial lipid-based reagents[23]. Herein, we have characterized the performance of siRNA-PA relative to unmodified siRNA delivered via endosomolytic, polymer-based NPs that have previously demonstrated efficacy both *in vitro* and for local scaffold-based delivery *in vivo*[25, 29]. The goal was to improve the potency and longevity of action of the siRNA and to reduce the potential for negative side effects in ultimate scaffold-based siRNA-NP delivery applications.

The siRNA-PA was successfully synthesized using a one-step reaction and purified using HPLC (Figure 1). An important advantage of siRNA-PA over unmodified siRNA was its improved NP packaging. siRNA-PA completely loaded into the NPs at a 4:1 N:P ratio, while unmodified siRNA necessitated a 6:1 ratio for the polymer utilized in these studies (Figure 2). These data suggest that hydrophobization of siRNA is an efficient means to improve siRNA cargo loading and stability of NPs[36]. Other reports that nanoparticle carriers loaded with lipid-modified siRNA form particles at lower N:P ratios and with increased stability also support this conclusion[45, 47, 48]. It is posited that interactions among siRNA molecules through the lipophilic moieties increase negative charge density by localizing multiple siRNA molecules; this grouping is proposed to improve loading by cationic agents[45, 49]. Additionally, aggregated lipophilic moieties contribute to micelle stability[48]. Another potential contributing factor, in our NP carriers in particular, is that the PA molecule may help to anchor the siRNA into the hydrophobic micellar nanoparticle core. These hydrophobic interactions could help to reinforce the electrostatic interactions between the siRNA and the poly(DMAEMA)-based NP corona. This hypothesis is supported by the finding that siRNA-PA NPs had larger hydrodynamic diameter than siRNA NPs (Figure 3), while unloaded NPs and siRNA NPs were the same size (data not

shown). These data suggest that siRNA-PA impacts the overall NP packing, potentially due to increased interaction with the NP core.

Next, siRNA-PA NP silencing of both the model gene luciferase and of the therapeutically relevant gene PHD2 was benchmarked against siRNA NPs in fibroblasts. Similar studies were also done in MSCs, which have relevance for tissue regenerative applications and represent a cell type that is notoriously challenging to transfect[31, 50]. The first study assessed the effects of the N:P ratio used in the NP formulation on luciferase silencing in fibroblasts. At every N:P ratio tested for an siRNA dose of 40 nM, siRNA-PA NPs produced significantly greater gene silencing than unmodified siRNA NPs (Figure 4). The largest improvement in silencing by siRNA-PA occurred at the lower N:P ratios of 1:1, 2:1, and 4:1. Beyond a ratio of 4:1, increasing the amount of polymer had no significant impact on target knockdown for siRNA-PA NPs. Achieving potent silencing with a lower N:P is key to minimizing detrimental treatment effects, as a charge ratio of 6:1 began to cause increased cytoxicity in fibroblasts (Figure S2). The siRNA-PA NPs achieved a high level (more than 70%) of silencing efficacy even at an N:P of 1:1, which was superior to unmodified siRNA loaded at a 4:1 N:P ratio (the standard formulation condition for this polymeric NP composition)[24, 29].

Gene silencing potency was also compared for the siRNA-PA NPs and unmodified siRNA NPs formed at a constant N:P of 4:1. In fibroblasts, the dose of siRNA-PA NPs required to achieve 50% gene silencing was consistently two- to three-fold lower than the dose of siRNA NPs needed to achieve this effect. The improved potency of siRNA-PA NPs was apparent both for the model gene luciferase and for the therapeutically-relevant gene PHD2 (Figure 5A, 6). An even greater increase in gene silencing potency of more than three-fold was observed in MSCs (Figure 5B). The polymer NPs used here have been shown to be promising for siRNA delivery to

MSCs[34], while commercial reagents like Lipofectamine and Dharmafect have substantial cytotoxicity and low transfection efficiencies[34, 40]. Our results suggest that there is a synergistic effect between this polymeric carrier and PA-siRNA for transfection of MSCs, which reinforces findings that PA modification of polymeric carriers enhanced MSC plasmid transfection[40]. Unlike strategies to increase bioactivity by increasing the polymer:siRNA N:P ratio, the siRNA conjugated to PA did not have any impact on cell viability. Because the siRNA-PA conjugation decreases the amount of polymer needed and also increases the relative potency of the siRNA, it has the potential to strongly impact the therapeutic index for polymeric NP siRNA formulations.

In order to better understand the mechanism for the improved gene silencing performance of siRNA-PA NPs, cellular uptake and intracellular retention were measured by flow cytometry. The results revealed a 35-fold increase in cellular uptake of DNA-PA NPs relative to DNA NPs in fibroblasts. This effect is attributable to the presence of PA moieties, which may hydrophobically interact with cell membranes. Endogenous PA modification of proteins facilitates membrane binding and endocytotic processes[39, 41], and the number of lipophilic modifications on nucleic acids directly correlates to the level of association with cell membranes[49]. Therefore, the presence of multiple PA moieties on the corona of the NPs may act cooperatively to facilitate uptake, in combination with the positive zeta potential of the NPs. Previous studies of PA-modified siRNA employing Lipofectamine 2000 as a delivery agent showed more modest improvements in cellular uptake relative to the gains achieved herein with polymeric NPs[20]. This discrepancy is likely attributable to differences in the mechanism of siRNA complexation or cellular internalization achieved with each type of reagent. For example, cholesterol-modified siRNA loaded into cationic polymer micelles also demonstrated moderate cellular uptake enhancement over unmodified siRNA in comparison to the improvement with

siRNA-PA over siRNA in our system[47]. However, in this system, lipophilic siRNA was packaged in the core of the micelles, whereas our NP carriers load siRNA/siRNA-PA onto the micelleplex corona, potentially promoting multivalent PA interactions with the cell membrane.

Investigation into the uptake mechanism of PA-conjugated oligo NPs revealed a larger role for macropinocytotic uptake in comparison to clathrin and caveolin-mediated endocytosis, as seen by the lack of uptake inhibition by Dynasore in comparison to EIPA and cytochalasin D (Figure 8). It is hypothesized that the PA modification facilitates strong uptake enhancement by preferentially accessing macropinocytotic pathways; this preferential uptake by macropinocytosis could be due to the larger size of the siRNA-PA NPs. Internalization via this pathway may also impact siRNA-PA NP intracellular retention and cytoplasmic bioavailability, as it is accepted that the endocytotic mechanism has a significant impact on the trafficking and ultimate intracellular fate of internalized therapeutics[51, 52]. For example, macropinosomes are believed to be leakier and to provide an easier access point into the cellular cytoplasm[52], which may enhance the efficiency of endosomal escape and intracellular bioavailability of the siRNA-PA NPs. These uptake inhibitor data, combined with the belief that PA conjugation improves siRNA resistance to degradation[20], motivated investigation of intracellular retention (Figure 7) and longevity of gene silencing (Figure 9). Both of these studies suggested significantly greater persistence for siRNA-PA NPs relative to siRNA NPs. This effect is anticipated to be impactful for regenerative applications where repeat administration of siRNA may not be convenient or feasible.

In conclusion, these studies indicated that siRNA conjugation to PA acts synergistically with endosomolytic polymer NP formulations. PA conjugation reduced the required ratio of polymer:siRNA and improved silencing potency, which was relevant across multiple genes and

cell types relevant to tissue regeneration. Ultimately, the siRNA-PA would significantly reduce the ratio of polymer:siRNA as well as the overall dose of siRNA necessary for functional gene silencing. Furthermore, PA conjugation significantly improved longevity of silencing of siRNA. Thus, utilization of siRNA-PA NPs would facilitate a sustained functional effect with less frequent and/or lower doses, effectively broadening the therapeutic index and enhancing the probability of success for siRNA applications in tissue engineering.

Future Work

Ongoing work concentrates on verifying the gene silencing and functional efficacy of the siRNA-PA nanoparticle system for local delivery via biomaterial scaffolds *in vivo*. This will be evaluated in a mouse subcutaneous implant model, which our lab has previously validated[25]. Future studies will also investigate the potential for siRNA conjugates to elicit local gene silencing effects without the use of a nanocarrier system.

REFERENCES

1. Sen, C.K. et al. Human skin wounds: a major and snowballing threat to public health and the economy. *Wound repair and regeneration : official publication of the Wound Healing Society [and] the European Tissue Repair Society* **17**, 763-771 (2009).
2. Duvall, C.L., Taylor, W.R., Weiss, D., Wojtowicz, A.M. & Guldberg, R.E. Impaired angiogenesis, early callus formation, and late stage remodeling in fracture healing of osteopontin-deficient mice. *Journal of bone and mineral research : the official journal of the American Society for Bone and Mineral Research* **22**, 286-297 (2007).
3. Duvall, C.L., Taylor, R. W., Weiss, D., Guldberg, R. E. Quantitative microcomputed tomography analysis of collateral vessel development after ischemic injury. *American Journal of Physiology - Heart and Circulatory Physiology* **287**, H302-H310 (2004).
4. Falanga, V. Wound healing and its impairment in the diabetic foot. *The Lancet* **366**, 1736-1743 (2005).
5. Maxson, S., Lopez, E.A., Yoo, D., Danilkovitch-Miagkova, A. & Leroux, M.A. Concise review: role of mesenchymal stem cells in wound repair. *Stem cells translational medicine* **1**, 142-149 (2012).
6. Hehehberger, K., Helborn, J. D., Brismar, K., Hansson, A. Inhibited proliferation of fibroblasts derived from chronic diabetic wounds and normal dermal flbroblasts treated with high glucose is associated with increased formation of L-lactate. *Wound Repair and Regeneration* **6** (1998).
7. Cheema, S.K., Chen, E., Shea, L.D. & Mathur, A.B. Regulation and guidance of cell behavior for tissue regeneration via the siRNA mechanism. *Wound repair and regeneration : official publication of the Wound Healing Society [and] the European Tissue Repair Society* **15**, 286-295 (2007).
8. Semenza, G.L. Regulation of oxygen homeostasis by hypoxia-inducible factor 1. *Physiology* **24**, 97-106 (2009).
9. Agis, H., Watzek, G. & Gruber, R. Prolyl hydroxylase inhibitors increase the production of vascular endothelial growth factor by periodontal fibroblasts. *Journal of periodontal research* **47**, 165-173 (2012).
10. Ceradini, D.J. et al. Progenitor cell trafficking is regulated by hypoxic gradients through HIF-1 induction of SDF-1. *Nature medicine* **10**, 858-864 (2004).
11. Wang, J., Lu, Z., Wientjes, M.G. & Au, J.L. Delivery of siRNA therapeutics: barriers and carriers. *The AAPS journal* **12**, 492-503 (2010).
12. Whitehead, K.A., Langer, R. & Anderson, D.G. Knocking down barriers: advances in siRNA delivery. *Nature reviews. Drug discovery* **8**, 129-138 (2009).
13. Murthy, N., Campbell, J., Fausto, N., Hoffman, A.S. & Stayton, P.S. Design and synthesis of pH-responsive polymeric carriers that target uptake and enhance the intracellular delivery of oligonucleotides. *Journal of Controlled Release* **89**, 365-374 (2003).
14. Akhtar, S. & Benter, I. Toxicogenomics of non-viral drug delivery systems for RNAi: potential impact on siRNA-mediated gene silencing activity and specificity. *Advanced drug delivery reviews* **59**, 164-182 (2007).
15. Falamarzian, A. et al. Effective down-regulation of signal transducer and activator of transcription 3 (STAT3) by polyplexes of siRNA and lipid-substituted polyethyleneimine for sensitization of breast tumor cells to conventional chemotherapy. *Journal of biomedical materials research. Part A* **102**, 3216-3228 (2014).

16. Kim, J., Sunshine, J. C., Green, J. J. Differential Polymer Structure Tunes Mechanism of Cellular Uptake and Transfection Routes of Poly(β-amino ester) Polyplexes in Human Breast Cancer Cells. *Bioconjugate chemistry* **25** (2014).
17. Nelson, C.E., Kintzing, R. J., Hanna, A., Shannon, J. M., Gupta, M. K., Duvall, C. L. Balancing Cationic and Hydrophobic Content of PEGylated siRNA Polyplexes Enhances Endosome Escape, Stability, Blood Circulation Time, and Bioactivity in Vivo. *ACS Nano* **7**, 8870-8880 (2013).
18. Ambardekar, V.V. et al. The modification of siRNA with 3' cholesterol to increase nuclease protection and suppression of native mRNA by select siRNA polyplexes. *Biomaterials* **32**, 1404-1411 (2011).
19. Nishina, K. et al. Efficient in vivo delivery of siRNA to the liver by conjugation of alpha-tocopherol. *Molecular therapy : the journal of the American Society of Gene Therapy* **16**, 734-740 (2008).
20. Kubo, T., Takei, Y., Mihara, K., Yanagihara, K. & Seyama, T. Amino-modified and lipid-conjugated dicer-substrate siRNA enhances RNAi efficacy. *Bioconjugate chemistry* **23**, 164-173 (2012).
21. Kubo, T. et al. Gene-Silencing Potency of Symmetric and Asymmetric Lipid-Conjugated siRNAs and Its Correlation with Dicer Recognition. *Bioconjugate chemistry* **24**, 2045-2057 (2013).
22. Kubo, T. et al. SiRNAs conjugated with aromatic compounds induce RISC-mediated antisense strand selection and strong gene-silencing activity. *Biochemical and biophysical research communications* **426**, 571-577 (2012).
23. Kubo, T. et al. Lipid-conjugated 27-nucleotide double-stranded RNAs with dicer-substrate potency enhance RNAi-mediated gene silencing. *Molecular pharmaceutics* **9**, 1374-1383 (2012).
24. Nelson, C.E. et al. Sustained local delivery of siRNA from an injectable scaffold. *Biomaterials* **33**, 1154-1161 (2012).
25. Nelson, C.E. et al. Tunable delivery of siRNA from a biodegradable scaffold to promote angiogenesis in vivo. *Advanced materials* **26**, 607-614, 506 (2014).
26. Gilleron, J. et al. Image-based analysis of lipid nanoparticle-mediated siRNA delivery, intracellular trafficking and endosomal escape. *Nature biotechnology* **31**, 638-646 (2013).
27. Tseng, Y.C., Mozumdar, S. & Huang, L. Lipid-based systemic delivery of siRNA. *Advanced drug delivery reviews* **61**, 721-731 (2009).
28. Layzer, J.M. In vivo activity of nuclease-resistant siRNAs. *Rna* **10**, 766-771 (2004).
29. Convertine, A.J., Benoit, D.S., Duvall, C.L., Hoffman, A.S. & Stayton, P.S. Development of a novel endosomolytic diblock copolymer for siRNA delivery. *Journal of controlled release : official journal of the Controlled Release Society* **133**, 221-229 (2009).
30. Rettig, G.R. & Behlke, M.A. Progress toward in vivo use of siRNAs-II. *Molecular therapy : the journal of the American Society of Gene Therapy* **20**, 483-512 (2012).
31. Tzeng, S.Y., Hung, B.P., Grayson, W.L. & Green, J.J. Cystamine-terminated poly(beta-amino ester)s for siRNA delivery to human mesenchymal stem cells and enhancement of osteogenic differentiation. *Biomaterials* **33**, 8142-8151 (2012).
32. Frank-Kamenetsky, M. et al. Therapeutic RNAi targeting PCSK9 acutely lowers plasma cholesterol in rodents and LDL cholesterol in nonhuman primates. *Proceedings of the National Academy of Sciences of the United States of America* **105**, 11915-11920 (2008).

33. Coelho, T. et al. Safety and efficacy of RNAi therapy for transthyretin amyloidosis. *The New England journal of medicine* **369**, 819-829 (2013).
34. Benoit, D.S. & Boutin, M.E. Controlling mesenchymal stem cell gene expression using polymer-mediated delivery of siRNA. *Biomacromolecules* **13**, 3841-3849 (2012).
35. Wu, S.Y. & McMillan, N.A. Lipidic systems for in vivo siRNA delivery. *The AAPS journal* **11**, 639-652 (2009).
36. Wei, H. et al. Dual responsive, stabilized nanoparticles for efficient in vivo plasmid delivery. *Angewandte Chemie* **52**, 5377-5381 (2013).
37. Nakayama, T. et al. Harnessing a physiologic mechanism for siRNA delivery with mimetic lipoprotein particles. *Molecular therapy : the journal of the American Society of Gene Therapy* **20**, 1582-1589 (2012).
38. Soutschek, J., Akinc, A., Bramlage, B., Charisse, K., Constien, R., Donoghue, M., Elbashir, S., Geick, A., Hadwiger, P., Harborth, J., John, M., Kesavan, K., Lavine, G., Pandey, R. K., Racie, T., & Rajeev, K.G., Rohl, I., Toudjarska, I., Wang, G., Wuschko, S., Bumcrot, D., Koteliansky, V., Limmer, S., Manoharan, M., Vornlocher, H. Therapeutic silencing of an endogenous gene by systemic administration of modified siRNAs. *Nature* **432** (2004).
39. Resh, M.D. Myristylation and Palmitylation of Src Family Members: The Fats of the Matter. *Cell* **76**, 411-413 (1994).
40. Clements, B.A., Incani, V., Kucharski, C., Lavasanifar, A., Ritchie, B., Uludag, H. A comparative evaluation of poly-L-lysine-palmitic acid and Lipofectamine 2000 for plasmid delivery to bone marrow stromal cells. *Biomaterials* **28**, 4693-4704 (2007).
41. Pearce, E.J., Magee, A. I., Smithers, S. R., Simpson, A. J. G. Sm25, a major schistosome tegumental glycoprotein, is dependent on palmitic acid for membrane attachment. *The EMBO Journal* **10**, 2741-2746 (1991).
42. Shen, X., Wan, C., Ramaswamy, G., Mavalli, M., Wang, Y., Duvall, C. L., Deng, L. F., Guldberg, R. E., Eberhart, A., Clemens, T. L., Gilbert, S. R. Prolyl Hydroxylase Inhibitors Increase Neoangiogenesis and Callus Formation following Femur Fracture in Mice. *Journal of Orthopaedic Research* (2009).
43. HoWangYin, K.Y. et al. HIF-prolyl hydroxylase 2 inhibition enhances the efficiency of mesenchymal stem cell-based therapies for the treatment of critical limb ischemia. *Stem cells* **32**, 231-243 (2014).
44. Evans, B.C. et al. Ex Vivo Red Blood Cell Hemolysis Assay for the Evaluation of pH-responsive Endosomolytic Agents for Cytosolic Delivery of Biomacromolecular Drugs. e50166 (2013).
45. Liu, H. et al. SiRNA-phospholipid conjugates for gene and drug delivery in cancer treatment. *Biomaterials* **35**, 6519-6533 (2014).
46. Alam, M.R. et al. Multivalent cyclic RGD conjugates for targeted delivery of small interfering RNA. *Bioconjugate chemistry* **22**, 1673-1681 (2011).
47. Oe, Y. et al. Actively-targeted polyion complex micelles stabilized by cholesterol and disulfide cross-linking for systemic delivery of siRNA to solid tumors. *Biomaterials* **35**, 7887-7895 (2014).
48. Oba, M. et al. Polyplex micelles prepared from omega-cholesteryl PEG-polycation block copolymers for systemic gene delivery. *Biomaterials* **32**, 652-663 (2011).

49. Schade, M., Berti, D., Huster, D., Herrmann, A. & Arbuzova, A. Lipophilic nucleic acids--a flexible construction kit for organization and functionalization of surfaces. *Advances in colloid and interface science* **208**, 235-251 (2014).
50. Haleem-Smith, H., Derfoul, A., Okafor, C., Tuli, R., Olsen, D., Hall, D. J., Tuan, R. S. Optimization of High-Efficiency Transfection of Adult Human Mesenchymal Stem Cells In Vitro. *Molecular Biotechnology* **30** (2005).
51. Reilly, M.J., Larsen, J.D. & Sullivan, M.O. Polyplexes traffic through caveolae to the Golgi and endoplasmic reticulum en route to the nucleus. *Molecular pharmaceutics* **9**, 1280-1290 (2012).
52. Khalil, I.A., Kogure, K., Akita, H. & Harashima, H. Uptake pathways and subsequent intracellular trafficking in nonviral gene delivery. *Pharmacological reviews* **58**, 32-45 (2006).

APPENDIX

Supplementary figures

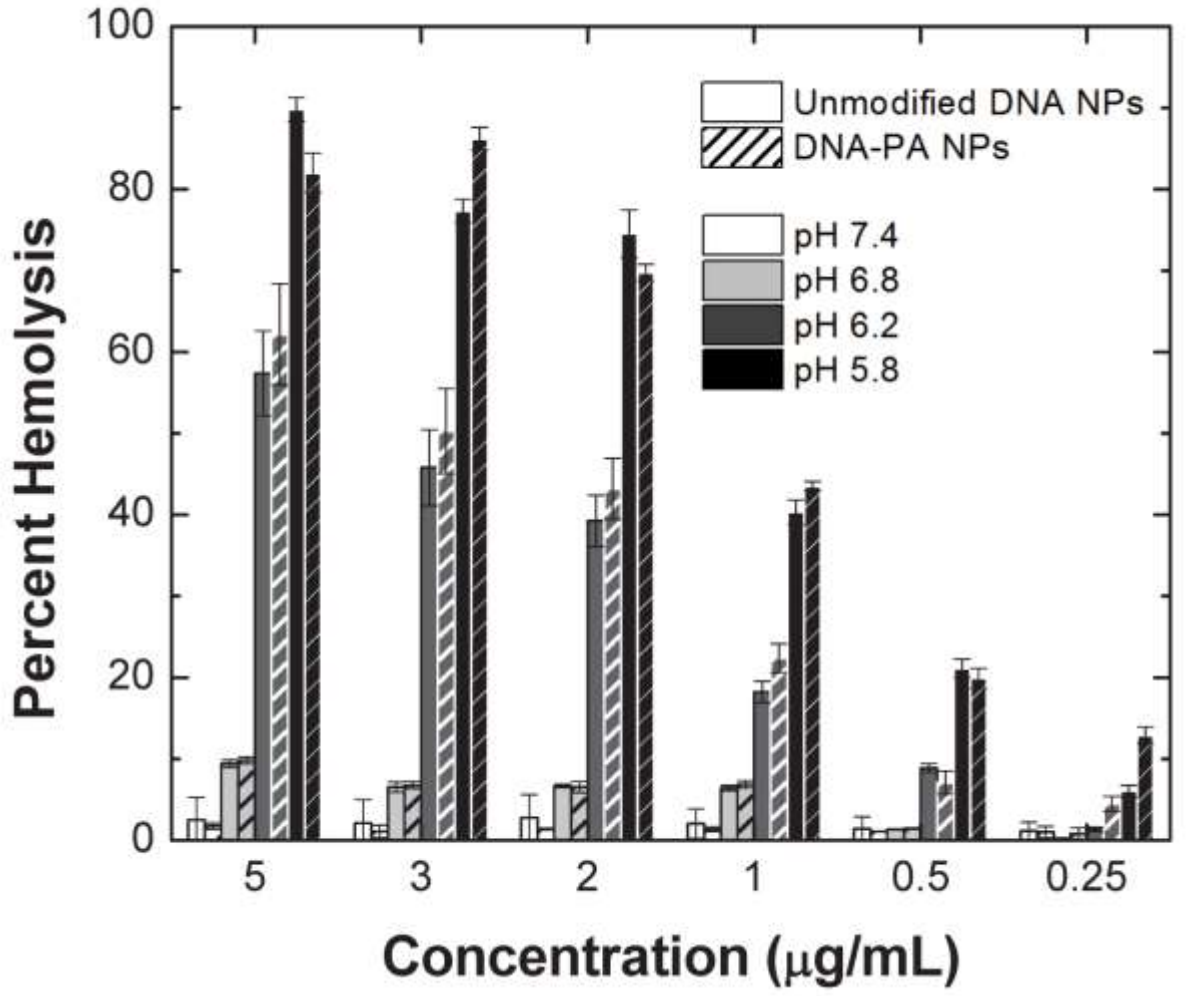

Figure S1. DNA vs. DNA-PA NPs showed no difference in pH- responsive, membrane-disruptive activity, as determined via red blood cell hemolysis assay.

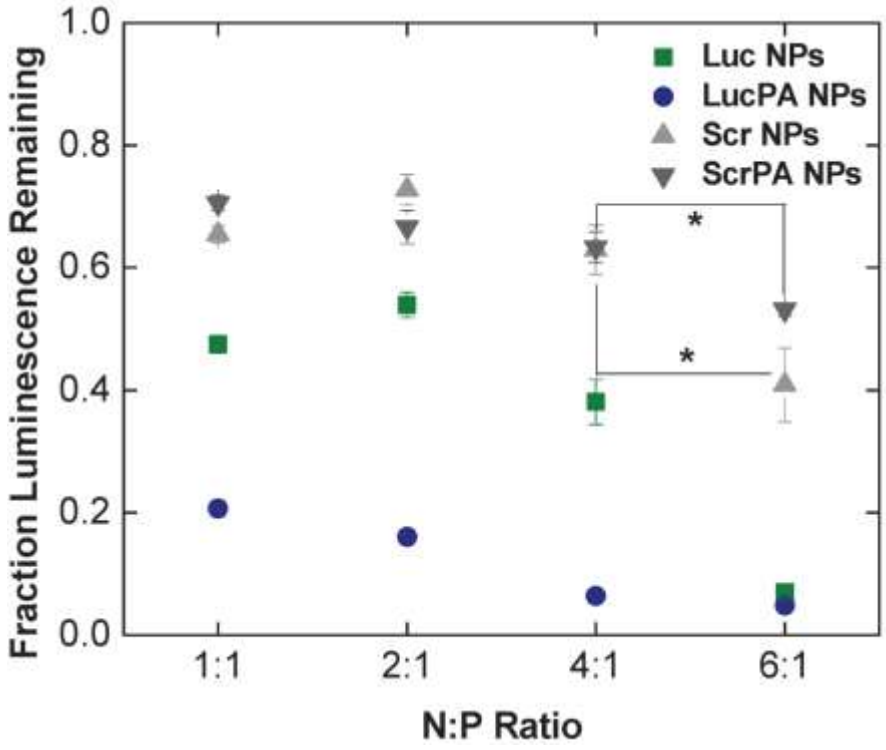

Figure S2. Significant increase in cytotoxicity using an N:P ratio of 6:1 vs. 4:1. These studies were done at 40 nM siRNA treatment for 24 hours in NIH-3T3 fibroblasts. Data are normalized to no treatment controls. *$p<0.05$ for scr, scr-PA NPs at a ratio of 4:1 vs. 6:1.

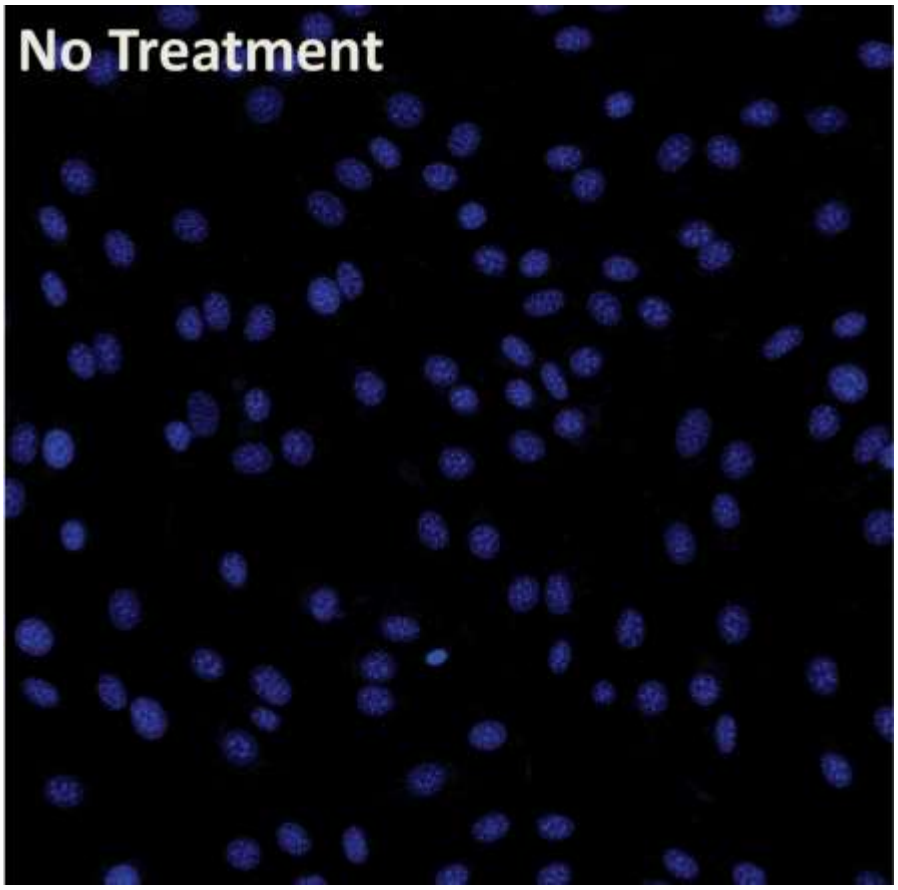

Figure S3. No background fluorescence observed in untreated fibroblasts. Shown is an image of untreated fibroblasts using the settings of the reported images showing fluorescence due to DNA NP and DNA-PA NP uptake.